J. Min. Metall. Sect. B-Metall. 52 (1) B (2016) 35 - 40

Journal of Mining and Metallurgy, Section B: Metallurgy

DISSOLUTION MECHANISM OF Al_2O_3 IN REFINING SLAGS CONTAINING Ce_2O_3

L.J. Wang [a,b,*], Q. Wang [a,b], J.M. Li [c], K.C. Chou [a,b]

[a] State Key lab of Advanced Metallurgy, University of Science and Technology Beijing, China
[b] Dept. of Physical chemistry, School of Metallurgical and Ecological Engineering, University of Science and Technology Beijing, China
[c] Taiyuan Iron & Steel Group Co., Ltd., Shanxi, China

(Received 06 July 2014; accepted 19 December 2015)

Abstract

In the present work, the rate of dissolution of Al_2O_3 rod in $CaO-SiO_2-Al_2O_3$ and $CaO-SiO_2-Al_2O_3-Ce_2O_3$ slags were carried out in the temperature range of 1793 K (1520 °C) - 1853 K (1580 °C) under static conditions. The cross section of the rod and the boundary layers were identified and analyzed by SEM-EDS. The dissolution of Al_2O_3 was favored with the increasing CaO/Al_2O_3 ratio, elevating temperatures as well as the addition of Ce_2O_3. An intermediate product $3CaO5Al_2O_3Ce_2O_3$ was detected. The mechanism of dissolution of Al_2O_3 in the Ce_2O_3 containing slag were also proposed as three steps involved: 1) the formation of calcium aluminates $CaO{\cdot}Al_2O_3$ at the interface 2) the formation of $3CaO5Al_2O_3Ce_2O_3$ as the reaction progresses; and 3) the dissolution of $3CaO5Al_2O_3Ce_2O_3$ into the slag.

Keywords: *Clean steel; Dissolution rate; Inclusions; Alumina; Refining slag; Ce_2O_3.*

1. Introduction

The importance of the removal of non-metallic inclusions has been realized in recent years as the demand for clean steel is increasing. Fast dissolution of non-metallic inclusions into molten slag during secondary steelmaking process would minimize the population and the size of nonmetallic inclusions in steel products. Thus, optimization of refining slag becomes even more important.

Regarding the typical inclusion, *viz.* Al_2O_3 in steel, a great amount of studies [1-13] have been carried out on the dissolution behavior of alumina into slags ($CaO-MgO-Al_2O_3-SiO_2-CaF_2-Na_2O$ etc.), especially on clarification of the dissolution mechanism. Two rate-determining steps have been proposed related to two kinds of dissolving phenomena: 1) the mass transfer in boundary layer of slag if no compound layer is formed, for example in Na_2O-SiO_2 system; 2) diffusion in solid compound layer if the dense compound layer such as $CaO.6Al_2O_3$, $MgO.Al_2O_3$ formed between alumina/slag interface. However, the refining slag containing Ce_2O_3 is not involved in above discussions.

Ce is known to be effective deoxidizer in making ultra-low oxygen steel in view of its strong affinity for oxygen and the deoxidation product, Ce_2O_3, would end up in the slag phase. And sometimes it is also used as an alloying element in stainless steel to improve the oxidation resistance. Ueda et al [14] have studied the activity of Al_2O_3 for the $CaO-Al_2O_3-Ce_2O_3$ system at 1773 K by a chemical equilibration technique. The result illustrated that the addition of Ce_2O_3 to the $CaO-Al_2O_3$ system decreased the activity and activity coefficient of Al_2O_3 in the melts. The viscosities of $RE_2O_3–MgO–SiO_2$ melts were found to decrease with increasing the content of any rare-earth oxide additions, Shimizu [15] has investigated the viscosity and surface tension of Ce_2O_3 slag, and found that Ce_2O_3 could lower the viscosity of the system at 1873 K.

Thus, in the present study, the dissolution of Al_2O_3 rod in the Ce_2O_3-containing slag was carried out in the temperature range of 1793 K - 1853 K under static conditions from the point of view of inclusion control.

2. Experimental

2.1 Sample Preparation

The compositions of slag samples used are listed in Table 1. The master slag was prepared from pure CaO, SiO_2, Al_2O_3, MgO and CeO_2. CaO was obtained by calcining $CaCO_3$ (Analytical grade) at 1373 K for 6h, and the rest oxides were dried at 1273 K for 4h. The powder sample was mixed in an agate mortar, pre-melted at 1873 K (1600 °C) in a resistance furnace for 1h in air, and then crushed into powder,

* *Corresponding author: lijunwang@ustb.edu.cn*

DOI:10.2298/JMMB140706004W

ready for measurements. In the present study, Al_2O_3 rod is used as Al_2O_3 inclusions, which dimensions are 6mm in diameter and 1000 mm in length measured by a micrometer in the accuracy of 1/1000 mm. The purity and density of Al_2O_3 rod are 99% and 3.765 g/cm^3, respectively.

Table 1. *Initial chemical compositions of slag (mass %)*

Slag	CaO (%)	Al_2O_3 (%)	SiO_2 (%)	Ce_2O_3 (%)	CaO/Al_2O_3
A	55.71	39.79	4.5	0	1.4
B	45.25	45.25	4.5	5	1
C	52.79	37.71	4.5	5	1.4
D	58.18	32.32	4.5	5	1.8
E	49.87	35.63	4.5	10	1.4

2.2 Experimental Apparatus and Procedure

A vertical $MoSi_2$ electric resistance furnace was used for the present studies. The temperature was regulated by a proportional integral differential (PID) controller. The corundum reaction tube used inside this furnace had the dimensions of OD 90mm, ID 80mm, length 1000mm. The furnace temperature was measured by a B-type thermocouple (Pt-30% Rh / Pt-6% Rh), where the deviation of temperature could be maintained within ± 1°C in the temperature even zone (10mm). Fig.1 shows the schematic diagram of the experimental apparatus employed in the present study.

The experiments were carried out in the temperature range of 1793 K-1853 K. In a typical run, 30g pre-melted slag sample was heated to the target temperature in a molybdenum crucible outside protected by a graphite crucible of 68mm in diameter and 100mm in length in the argon atmosphere. An alumina rod (6mm in diameter) was pre-heated above the slag surface for 10 min, subsequently immersed in the slag. After predetermined time, the rod was withdrawn from the slag and rapidly pulled out of the furnace. The slag layer adhering to the surface of the alumina rod was removed by dipping the same in HCl dilute solution. The diameter of the remaining alumina rod was measured six times at different places in the part that was dipped into the slag. From these values, the average diameter of the rod after the reaction was evaluated. The scatter in the measured values of the diameter was less the 1 % indicating the uniformity of erosion in all the directions. The morphology of the cross section was subjected to SEM observation with EDS analysis.

The dissolution experiments were conducted at 1793 K for different time interval for slag C. Some experiments were also conducted for slag C for 1h at temperatures of 1793, 1823, and 1853 K. For one of the experimental series, the slag composition was changed from A to E at 1823 K for a treatment time of 1h.

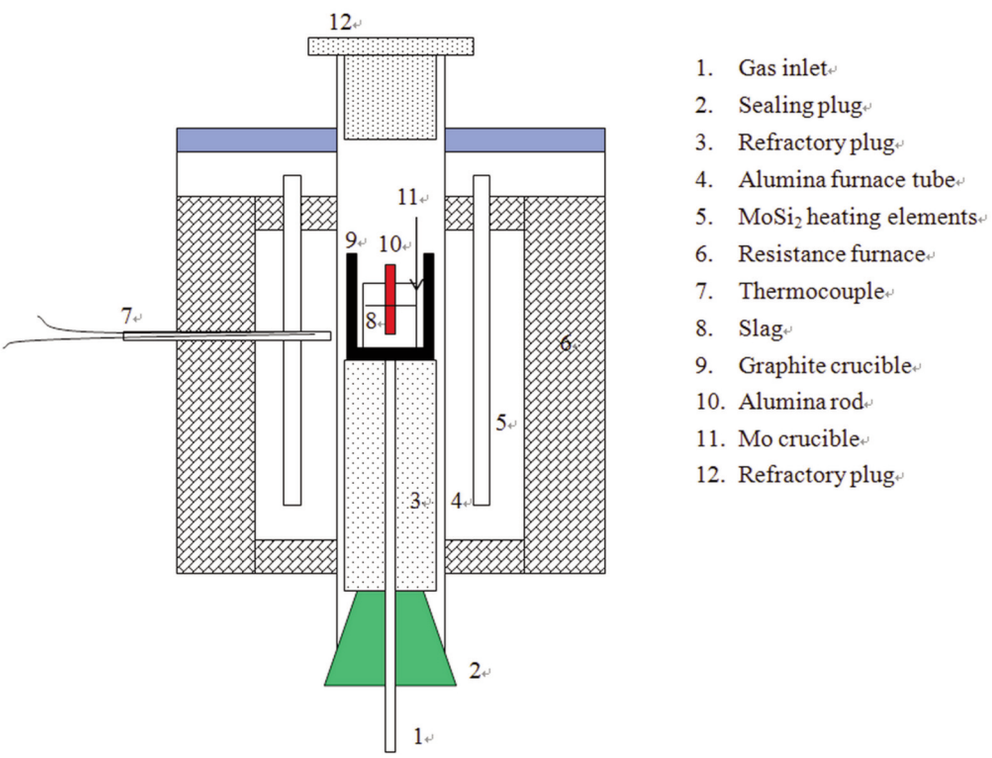

Figure 1. *Experimental setup*

3. Results

The cross section photomicrographs of two samples of the alumina rod corresponding to slag C at 1793K for 0.5h and 2h are shown in Figs 2 and 3. It is seen that there are two layer formed between pure Al_2O_3 and slag: a dark layer and a bright one. The composition of these two layers were identified by EDS analysis as calcium aluminate with varying Ca and Al contents, as well as Ce in outer layer. Fig. 4 shows EDS results for dark compound. In the outer layer, the compositions in the bright phase contain Ce-doped calcium aluminate, as shown in Fig.5. Moreover, the layer containing Ce has over-lapped the single calcium aluminate layer when dissolving time was extended. It is seen that the reaction is topochemical and the thickness of this product layer growing above the Al_2O_3 rod increases with time. Samples with exposure times in between had a similar behavior.

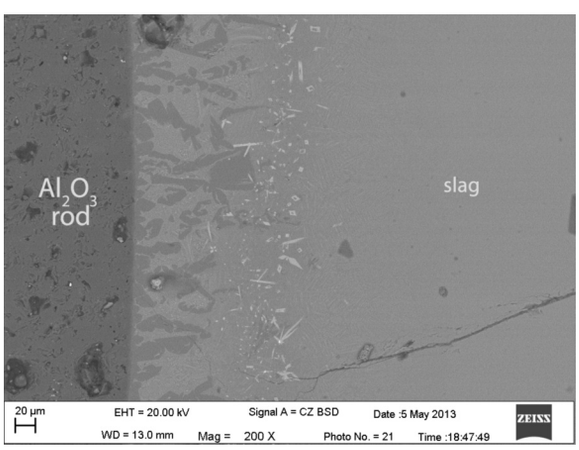

Figure 2. *Solid product layers between slag and Al_2O_3 in slag C at 1793K for 0.5h*

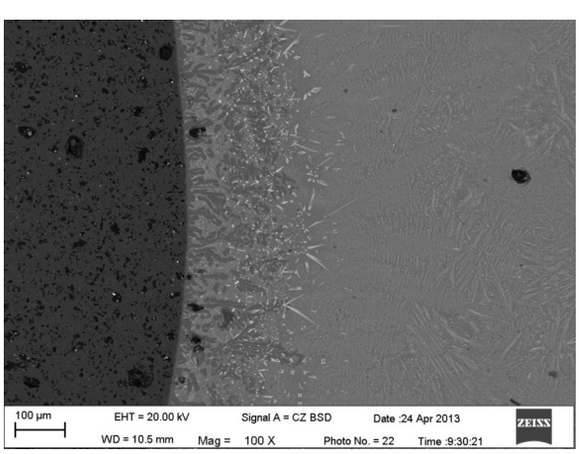

Figure 3. *Solid product layers between slag and Al_2O_3 in slag C at 1793K for 2h*

The decrease in the radius of the Al_2O_3 core with

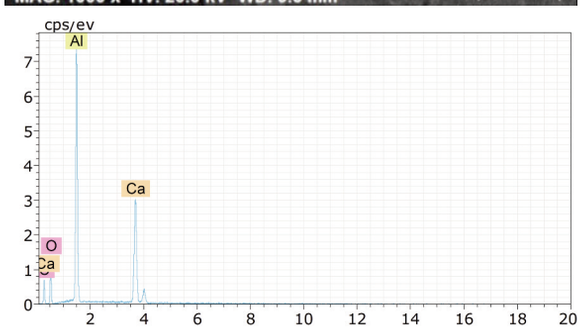

Figure 4. *EDS analysis results for the black product layer*

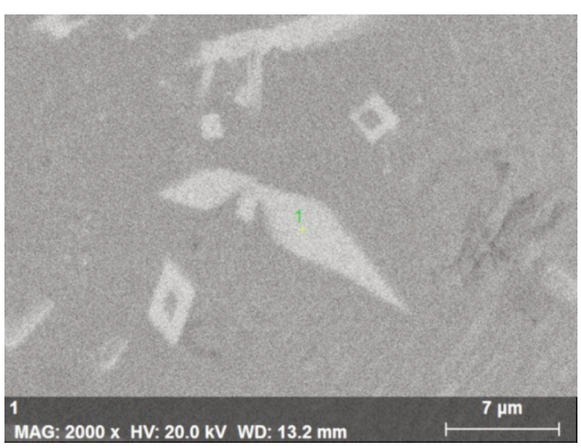

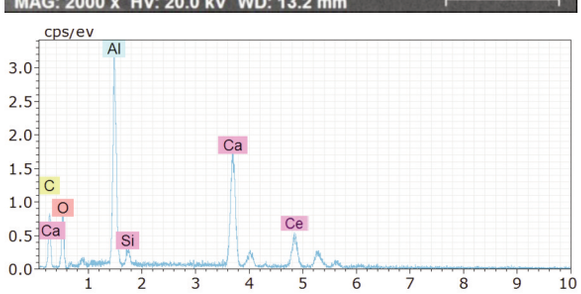

Figure 5. *EDS analysis results for the bright product layer*

Table 2. *Values of change in radius of Al_2O_3 rod and solid solution thickness in slag C at 1793 K*

t/h	ΔR/mm	ΔX/mm	ΔQ/mm	ΔL/mm	(ΔR-ΔX)/mm
0	0	0	0	0	0
0.5	0.3197	0.1255	0.0732	0.1654	0.2109
1	0.6243	0.1684	0.1755	0.2566	0.4839
2	1.0734	0.1942	0.22	0.3149	0.8422
3	1.6103	0.2271	0.1858	0.2604	1.4042

respect to the initial radius , ΔR in the case of slag C at different time intervals at 1793K, is presented in Table 2. The change of the formation layer thickness ΔX (black compound layer), ΔQ (the diffusion layer) and ΔL (formation layer + diffusion layer) for slag C are also given in the same table, respectively. Similar data for the variation of slag compositions at 1793K for 1h, as well as the influence of temperature on reaction in slag C for 1h are presented in Table 3 and Table 4.

From these data, it is found that Δx increases with time. A plot of ΔR as a function of t within 3h shows a linear relationship in Fig. 6, and the regression equation to this line was obtained as

$$\Delta x = 0.5251t \pm 0.043$$

where units of ΔR and t are mm and hour, respectively. As for the relationship between ΔR and t, a linear line is also obtained in Fig. 7 as a function of $t^{0.5}$ instead of t. The corresponding equation is.

$$\Delta x = 0.1291t^{0.5} \pm 0.017$$

Although the thickness of the outer layer was found to increase with time, similar figures describing a linear relationship as ΔQ- $t^{0.5}$ or ΔQ- t are not obtained. As can be seen in Fig. 8, the thickness of the outer layer, DQ, initially increases with time, and after 2h, becomes steady.

Table 3. *Values of change in radius of Al_2O_3 rod and the thicknesses of formation layer as well as the diffusion layer in slag C for 1h*

T/°C	ΔX/mm	ΔL/mm	ΔR/mm
1520	0.1684	0.1755	0.6243
1550	0.2259	0.1571	0.9819
1580	0.2832	0.1284	1.7394

Table 4. *Values of change in radius of Al_2O_3 rod and the thicknesses of formation layer as well as the diffusion layer at 1793K for 1h*

Slags	ΔX/mm	ΔL/mm	ΔR/mm
A	0.2854	0.2854	0.5997
B	0.3688	0.7811	0.4106
C	0.1404	0.2566	0.6243
D	0.1038	0.2734	0.8855
E	0.1906	0.9002	0.6169

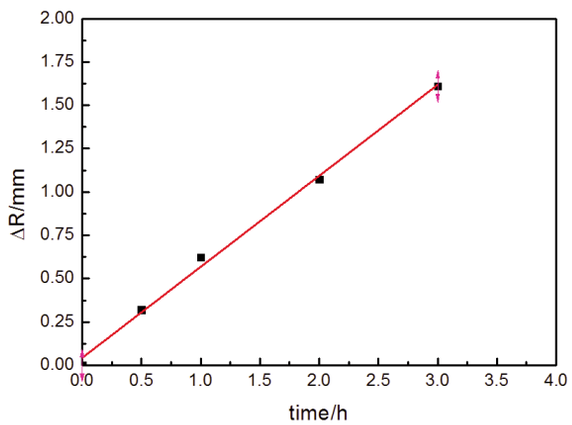

Figure 6. *Decrease of radius of Al_2O_3 (ΔR) as a function of time in slag C at 1793K*

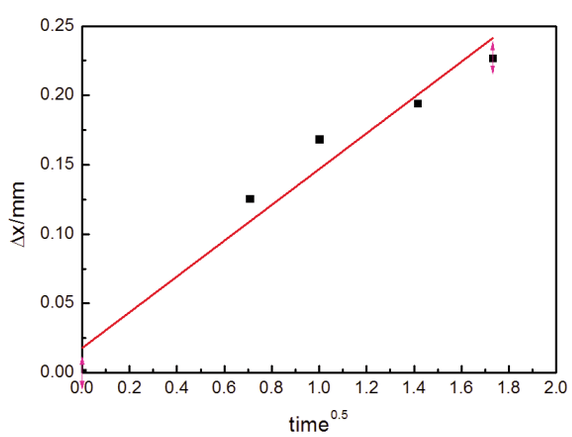

Figure 7. *Thickness of the inner layer (Δx) as a function of square root of time in slag C at 1793K*

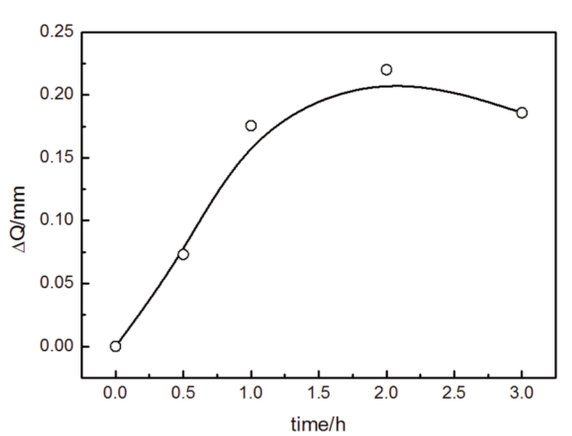

Figure 8. *Thickness of the outer layer (ΔQ) as a function of time in slag C at 1793K*

4. Discussions

4.1 Mechanism of Al_2O_3 dissolution in slags

The process of Al_2O_3 dissolution in a slag type used in the current study may be considered to consist of the following steps: a) the formation of calcium aluminates $CaOAl_2O_3$ at the interface b) the formation of $3CaO5Al_2O_3Ce_2O_3$ as the reaction progresses; and c) the dissolution of $3CaO5Al_2O_3Ce_2O_3$ into the slag. Taira [2] and Choi [3] have investigated the dissolution behavior of alumina rod into CaO-Al_2O_3-SiO_2 slag system, and found the formation of $CaO2Al_2O_3$ in the boundary between slag and alumina rod. In the present case, the formation of $CaOAl_2O_3$ on the surface of Al_2O_3 rod is attributed to the relative high CaO/Al_2O_3 ratio.

Phase diagram of CaO-Al_2O_3-Ce_2O_3 were replotted in Fig. 9, along with our experimental compositions with the fixed SiO_2 content. Ueda et. al confirmed the presentence of two ternary compounds $8CaO3Al_2O_33Ce_2O_3$ and $3CaO5Al_2O_3Ce_2O_3$ at 1773K in CaO-Al_2O_3-Ce_2O_3 ternary system. Although SiO_2 is contained in the present composition, the effect of SiO_2 on the dissolution can be neglected in view of its limited content (4.5%). Thus, the phase diagram of ternary CaO-Al_2O_3-Ce_2O_3 was used for discussion.

The growth rate of the solid compound layer is considered to be due to the counter diffusion of Ca^{2+} and Al^{3+} ions in a relatively rigid oxygen ion lattice. An effective parabolic rate constant for solid compound layer growth is obtained as 0.191 as shown in Fig. 7.

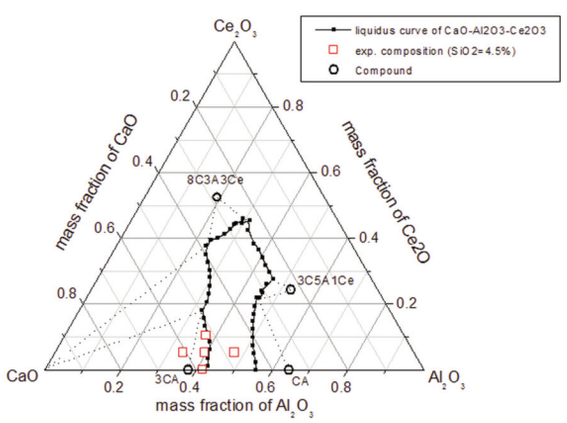

Figure 9. *Phase diagram of CaO-Al_2O_3-Ce_2O_3 at 1773K [14]*

4.2 Temperature dependence

According to the Arrhenius equation, the temperature dependence of the corrosion process can be written in

$$j = A\exp(-\frac{E}{RT}) \quad (1)$$

where E is the activation energy for the dissolution process. Meanwhile the diffusion flux also equals to $\rho_{Al_2O_3}\frac{\Delta R}{\Delta t}(g/cm^2\cdot s)$. Plots of the logarithm of $\frac{\Delta R}{\Delta t}$ as a function of the reciprocal temperature for the present results follow this behavior, as illustrated in Fig. 10. Regression analysis of the experimental data for slag C at different temperatures was carried out and the eqn.(2) was obtained with the standard error of 0.188.

$$\log j = \frac{24620}{T} + 10.56 \quad (2)$$

Comparison the eqn (1) and eqn (2), the activation energy is yields as 204 kJ/mol, which is close to the values 249-347 kJ/mol [17] obtained in the corresponding study under rotating conditions in spite of composition variety in two system.

A number of factors will influence the activation energy, such as diffusivity, viscosity as well as the content of Ce_2O_3 etc.

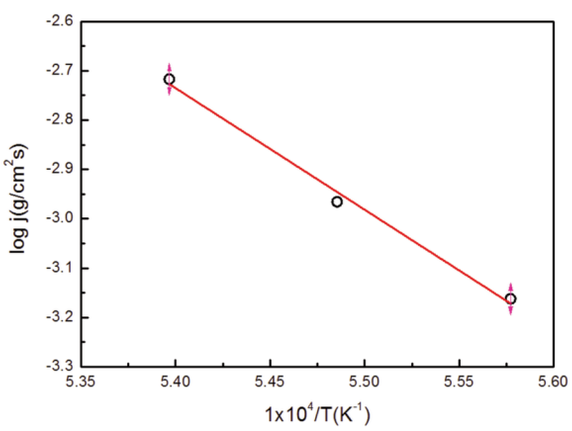

Figure 10. *Effect of temperature on the dissolution rate of Al_2O_3 in slag C for 1h*

4.3 The ratio of CaO/ Al_2O_3 dependence

As presented in Fig. 11, the variation of ΔR is increasing with the CaO/Al_2O_3, which implies that large ratio of CaO/ Al_2O_3 is beneficial to the dissolution rate of Al_2O_3 rod in slag. In order to figure out of the influence of CaO/ Al_2O_3 on each step, ΔL, and ΔX were also drawn in the Fig. 11. It can be found that the length of each "layer" is decreasing with the increasing the CaO/Al_2O_3 ratio first. Moreover, in the lower ratio of CaO/ Al_2O_3 from 1 to 1.4, the dissolution rate of Al_2O_3 is enhanced by the fast dissolution of $3CaO5Al_2O_3Ce_2O_3$ into slag, while further increasing CaO/Al_2O_3, such effect exhibited quite limited. The further increasing dissolution rate of Al_2O_3 lies in the increase of $3CaO5Al_2O_3Ce_2O_3$ formation layer.

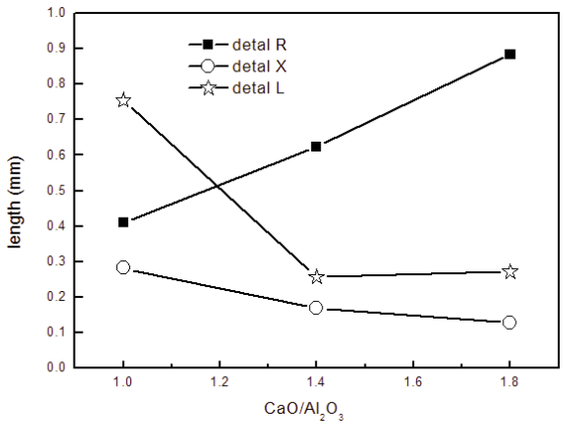

Figure 11. *Effect of CaO/Al_2O_3 on the dissolution of Al_2O_3 in slag (Ce_2O_3=5%) at 1793K for 1h*

4.4 Effect of Ce_2O_3 in slag

As shown in Fig.12, the dissolution rate of Al_2O_3 rod under static conditions was slightly improved when Ce_2O_3 added to the slag. The dissolution rate shows an initial increase followed by a downward trend. This is consistent with the previous investigation under forced convection (rotating rod) [15]. In order to analyze the function of Ce_2O_3, the variations of Δ x as well as the Δ L with the content of Ce_2O_3 was examined. As mentioned above, there are three parallel steps during the dissolution process. With addition of Ce2O3 in slag, the $3CaO5Al_2O_3Ce_2O_3$ forms, which reduce length of the CaO Al_2O_3 layer. And the total length of compound layer is also decreasing, which is contributed to the fast dissolution of $3CaO5Al_2O_3Ce_2O_3$. Since no liqudus temperatures of CaO-Al_2O_3-4.5%SiO_2-Ce_2O_3 are available, the dissolution driving force of $3CaO5Al_2O_3Ce_2O_3$ cannot be estimated. But based our previous study on the viscosity of CaO-MgO-Al_2O_3-SiO_2-Ce_2O_3, the addition of Ce_2O_3 would lower the viscosity, which is beneficial to the mass transfer in slag. This resulted in the increasing dissolution of Al_2O_3.

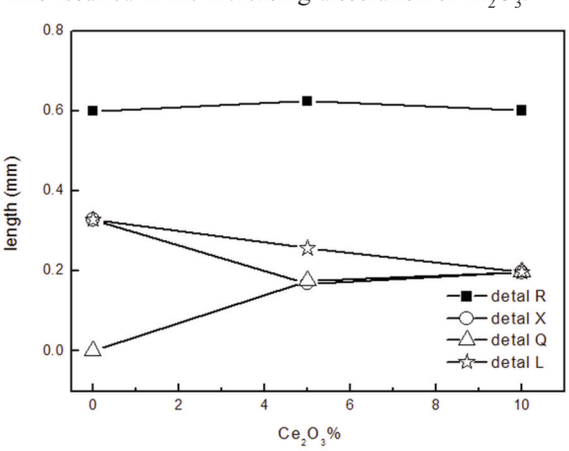

Figure 12. *Effect of Ce_2O_3 on the dissolution of Al_2O_3 in slag (CaO/Al_2O_3=1.4) at 1793K for 1h*

5. Conclusions

The mechanism of Al_2O_3 rod dissolved in CaO-Al_2O_3-SiO_2-Ce_2O_3 system has been studied at 1793, 1823, and 1853 K. The effect of temperature, ratio of CaO/Al_2O_3 as well as the Ce_2O_3 content on the dissolution behavior was examined. The dissolving process contains three parallel steps: $CaO.Al_2O_3$ formation - > $3CaO5Al_2O_3Ce_2O_3$layer formation - > dissolution of the $3CaO5Al_2O_3Ce_2O_3$. The dissolution rate of Al_2O_3 is favoured as the temperature of dissolution is increased. Further increases of the CaO/Al_2O_3 ratio and the amount of Ce_2O_3 in the slag can improve the dissolving rate then goes down afterwards slightly, which is consistent with the rotating dissolving results.

Acknowledgement

The authors would like to express their appreciation to the NSFC (No. 51104013, 51174022) and Beijing Higher Education Young Elite Teacher Project (No.0349) for the financial support of this research. The authors also express their sincere thanks to Professor Seshadri Seetharaman from Royal Institute of Technology Sweden for the valuable suggestions.

Reference

[1] W.D. Cho, P. Fan, ISIJ international, 44(2) (2004) 229-234.

[2] S. Taira, K. Nakashima, K. Mori, ISIJ international, 33(1) (1993) 116-123.

[3] J. Y. Choi, H. G. Lee, J. S. Kim, ISIJ international, 42(8) (2002) 852-860.

[4] M. Valdez, G. S. Shannon, S. Sridhar, ISIJ international, 46(3) (2006) 450-457.

[5] K.W. Yi, C. Tse, J.H. Park, M. Valdez, A.W. Cramb, S. Sridhar, Scandinavian journal of metallurgy, 32(4) (2003) 177-184.

[6] S. Sridhar, A. W. Cramb, Metall. Mater. Trans. B, 31B, (2000) 406-410.

[7] K.H. Sandhage, G.J. Yurek, J. Am. Ceram. Soc., 73 (1990) 3633-3642.

[8] K.H. Sandhage, G.J. Yurek, J. Am. Ceram. Soc., 73 (1990) 3643-3649.

[9] Y. Oishi, A.R. Cooper, W.D. Kingery, J. Am. Ceram. Soc., 48(2) (1965) 88-95.

[10] A.R. Cooper, W.D. Kingery, J. Am. Ceram. Soc., 47(1) (1964) 37-43.

[11] X. Yu, R. J. Pomfret,K. S. Coley, Metall. Mater. Trans. B, 28B (1997) 275-279.

[12] S. Zhang, H.R. Rezaie, H. Sarpoolaky and W. E. Lee, J. Am. Ceram. Soc., 83(4) (2000) 897-903.

[13] S. Ueda, K. Morita, N. Sano et. al., ISIJ international, 38(12) (1998) 1292-1296.

[14] F. Shimizu, H. Tokunaga, N. Saito, et al. ISIJ international, 46(3) (2006) 388-393.

[15] Y.Liu, L. Wang, K. Chou, ISIJ international, 46(3) (2014) 388-393.